Thermal conductivity of Si nanowires with δ-modulated dopant distribution by self-heated 3ω method and its length dependence

Fuwei Zhuge, Tsunaki Takahashi, Masaki Kanai, Kazuki Nagashima, Naoki Fukata, Ken Uchida, and Takeshi Yanagida

Citation: Journal of Applied Physics **124**, 065105 (2018); doi: 10.1063/1.5039988
View online: https://doi.org/10.1063/1.5039988
View Table of Contents: http://aip.scitation.org/toc/jap/124/6
Published by the American Institute of Physics

Thermal conductivity of Si nanowires with δ-modulated dopant distribution by self-heated 3ω method and its length dependence

Fuwei Zhuge,[1,a)] Tsunaki Takahashi,[2] Masaki Kanai,[2] Kazuki Nagashima,[2] Naoki Fukata,[3] Ken Uchida,[4] and Takeshi Yanagida[2,a)]
[1]*School of Materials Science and Engineering, Huazhong University of Science and Technology, Wuhan 430074, People's Republic of China*
[2]*Institute for Materials Chemistry and Engineering, Kyushu University, 6-1 Kasuga-Koen, Kasuga, Fukuoka 816-8580, Japan*
[3]*National Institute for Materials Science, 1-1 Namiki, Tsukuba, Ibaraki 305-0044, Japan*
[4]*Department of Electrical Engineering, Keio University, 3-14-1 Hiyoshi, Kouhokuku, Yokohama 223-8522, Japan*

(Received 13 May 2018; accepted 21 July 2018; published online 10 August 2018)

Here, we report the thermal conductivity measurement of B-doped Si nanowires with δ dopant modulation on the surface using the self-heated 3ω method, which resembles the thermal dissipation in operating electronic devices. The thermal conductivity for δ-modulated Si nanowires of 45 nm diameter ($\sim$23 W/m K) is found to agree well with that of non-doped Si nanowires reported previously, which is attributed to the dominant surface boundary scattering and the highly confined dopant distribution at the surface. Furthermore, through a length dependent study of the thermal conductivity (κ) from 400 nm to 4 μm, we found an apparent length dependence of κ at $L < 2\,\mu$m. The phenomenon could not be simply interpreted by solely considering the ballistic effect in thermal transport, but can be accounted for by including the additional resistive processes that are associated with the thermalization of joule-heating emitted phonons, which opts in to suppress the thermal conductivity of nano-systems under the ballistic thermal transport regime. *Published by AIP Publishing*. https://doi.org/10.1063/1.5039988

INTRODUCTION

Thermal engineering of nanostructured materials has attracted much attention due to their close relevance to thermoelectric applications and various kinds of nanodevices, including transistors,[1] light-emitting-diodes, and sensors.[2] Since the heat energy in semiconductors and dielectrics is mostly carried by phonons, understanding the phonon transport characteristics is critical for thermal engineering.[3] However, directly probing or measuring the essential phonon characteristics, including the frequency ω, specific heat C_p, propagating velocity v, and mean free path Λ, has been a universal challenge because the measurable thermal conductivity κ values always contain all these contributions from activated phonon modes in the Brillouin zone: $\kappa = 1/3 \sum C_{p,\omega} v_\omega \Lambda_\omega$, not to mention the complicated scattering processes that phonons experience, e.g., the scattering from impurities, surfaces, and interfaces. Many previous studies have focused on decreasing the thermal conductivity of nanostructured materials by the reduced size dimension in membranes,[4] nanowires,[5–7] and nanotubes.[8] For example, Si nanowires of the characteristic diameter of 20–100 nm in the radial direction have been demonstrated to exhibit 5–10 fold reduced thermal conductivity (15–30 W/m K) from the bulk value (148 W/m K),[5] which could be further decreased by engineering the surface roughness.[9] The explicit role of the surface in reducing the thermal conductivity has been extensively studied from both the experimental and theoretical perspectives.[10–13] However, few studies paid attention to the role of dopant impurities in the thermal conductivity of nanostructured materials with reduced dimensions, though they are universally present in electronic devices.

The dopant impurities are vital to the electrical properties of semiconductors. Engineering their distribution has been widely adopted to improve the electronic transport properties in nanostructured devices,[14] i.e., by using δ-profiled dopant distribution, the electron mobility in thin nanowires could be effectively enhanced.[15] For thermal carrying phonons, the presence of dopant impurities tends to decrease the thermal conductivity by the phonon scattering at mass disorder.[16,17] For example, in 3 μm thick Si membranes, the heavy B-doping $>10^{19}$ cm^{-3} decreases the thermal conductivity by 10%.[18] Although impurity doping or alloying is desired to reduce the thermal conductivity of materials in thermoelectric applications,[3] such an effect should be avoided in high power electronic devices because of the increasing concerns on overheating issues.[1,19] However, hitherto, few studies have paid attention to the effect of dopant impurities on the thermal conductivity of nanostructures. Recently, Pan *et al.* found experimentally that discrete surface doping of 100 nm Si nanowires by Ge leads to 23% reduction of nanowire thermal conductivity,[20] and the factor increases more by the diffusion of dopant atoms into the core of nanowires. This indicates that the distribution of dopant impurities in nanowires could be critical for the phonon transport. A reversal engineering of the dopant incorporation to surface boundaries seems promising and

a)Electronic addresses: zhugefw@hust.edu.cn and yanagida@cm.kyushu-u.ac.jp

practical to restrain the dopant impurity atoms from impeding the thermal transport in nanostructures.

In this work, we study the thermal conductivity of surface δ-modulated B-doped Si nanowires that exhibit an intrinsic core without impurity and a heavily B-doped surface layer. The self-heated 3ω method was employed to extract the thermal conductivity of nanowires in the 1D approximation considering its feasible deployment and close relevance to thermal dissipation situations in joule heated nanodevices.[21] Furthermore, we also explore the thermal conductivity of a series of δ-modulated B-doped Si nanowires with varied lengths within 0.4–4 μm to explore the effect of the longitudinal size restriction on the thermal transport and dissipation in Si nanowire devices.

RESULTS AND DISCUSSION

In order to measure the thermal conductivity, suspended Si nanowire devices were made to avoid unguarded thermal dissipation to the adjacent substrate. A schematic of the fabrication process is illustrated in Fig. 1(a). Briefly, a ~270 nm PMMA layer coated on the Si/SiO_2 substrate was used as the sacrificial layer and to support the nanowire in the beginning. The nanowire was then drop-cast on the as-made PMMA layer, followed by a standard electron-beam lithography (EBL) process. The electrode contacts to the nanowire were then made by using 20 nm Pt and 300 nm Au. Finally, the device was thoroughly rinsed in low viscosity hydrofluoroether (HFE, surface tension ~13.6 mN/m) solution before any significant solvent evaporation occurs to suppress detrimental capillary forces that tend to draw nanowire collapse to the substrate. Figure 1(b) displays the second electron microscopy (SEM) image of the as-prepared 4-termial device from the tilted view (top view in the inset). The floating height of nanowires is close to the initial thickness of the sacrificial PMMA layer. Different from any conventional Si nanowires, the present nanowires exhibit an intrinsic core without dopant impurities and a heavily B-doped surface layer, which were fabricated using the vapor-liquid-solid (VLS) method by controlling the temperature and the dopant source incorporation.[15] The nanowires exhibit an average diameter of 45 nm defined by the catalyst size. A high resolution transmission electron microscopy (HRTEM) image of the measured delta-doped nanowire is shown in Fig. 1(c). Below the surface oxide layer (~1.5 nm), a ~2 nm thin disordered crystalline layer was observed due to the high concentration incorporation of B atoms.

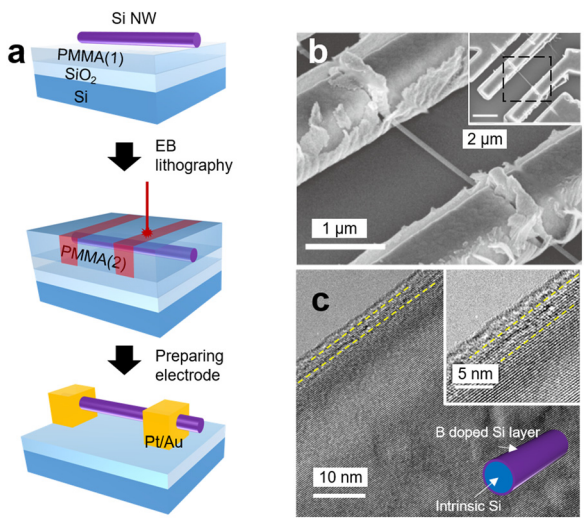

FIG. 1. (a) The fabrication process for the suspended Si nanowire device using the PMMA resist as the sacrificial layer. (b) SEM image of the fabricated 4-terminal device and (c) HRTEM image of the δ-doped Si nanowire with an intrinsic core but a heavily B-doped surface layer.

In the previous study, we have demonstrated that radial δ-modulation in B-doped Si nanowires could improve the hole mobility by alleviating the trapping and scattering from the surface,[15] while their impact on the thermal transport properties of nanowires is still unknown. Because of the heavy B-doping on the surface, we were able to achieve feasible ohmic contact to the nanowire using the Pt/Au electrode (width ~1 μm). The measured Si nanowires have resistivity in the range of 10^{-3}–10^{-2} Ω cm, corresponding to the dopant concentration of ~10^{18}–10^{19} cm^{-3} from field effect measurements.[15] In Fig. 2(a), we analyzed the contact resistance to nanowire using the 4-probe method, which is within ~1% to 10% of the total resistance of nanowire. As displayed in Fig. 2(b), the nanowire manifests an almost linear temperature coefficient of resistance (TCR, R'~72.5 Ω/K) in a wide temperature range, which is suitable for the calibration of the average temperature on the nanowire. In order to perform the 3ω measurement, which uses the third harmonic voltage oscillation to probe the thermal conductivity, a system based on a variable resistor, differential amplifiers, and a lock-in amplifier was customized. During measurement, the fabricated Si nanowire device was placed in an evacuated cryogenic chamber (pressure < 0.01 Pa), and

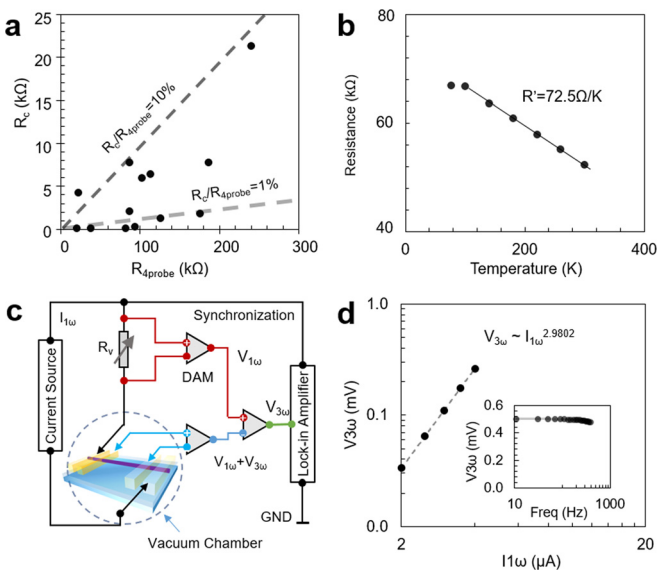

FIG. 2. (a) The electrical contact resistance (R_c) to Si nanowires compared to the measured 4-probe resistance of nanowires. (b) The temperature dependence of nanowire resistance for a δ-modulated B-doped Si nanowire showing the semiconductor like behavior. (c) The configuration of the customized 3ω measurement system, in which the suspended nanowire device is placed in an evacuated cryogenic chamber. (d) The measured $V_{3\omega} \sim I_{1\omega}$ relation by sweeping the current source amplitude under a constant frequency of 10 Hz (the inset shows the measured the frequency dependence of $V_{3\omega}$).

oscillating AC was then flowed in the circuit by using a current source (Keithley 6221). The variable resistance R_v was tuned to match the nanowire resistance R_{nw} to cancel the large ω voltage signal that may saturate the lock-in amplifier. The source current in measurement was swept from 2 to 10 μA to extract the 3ω voltage and then calculate the nanowire thermal conductivity using $\kappa = 4I_\omega{}^3RR'L/\pi^4V_{3\omega}S$,[21] in which L and S are, respectively, the length and cross section area of the nanowire and I_ω and $V_{3\omega}$ are the amplitude values of source current and measured voltage. In Fig. 2(d), the measured $V_{3\omega}$ at the source current frequency of 10 Hz is plotted versus $I_{1\omega}$, which is seen to follow an accurate $I_\omega{}^3$ dependence described by the above equation.[22] A frequency dependent measurement is shown in the inset of Fig. 2(d). The measured $V_{3\omega}$ voltage signal is generally saturated at a low frequency limit (<100 Hz). This behavior demonstrates that the measurement is quasi-static and the thermal dissipation in nanowires could be considered in the steady condition, which is required for the thermal conductivity determination in the 3ω method.[21]

We note that at higher frequencies, the measurements became more vulnerable to the parasitic capacitance (1–1.5 nF) effect in the circuit, which led to the rapid decrease in $V_{3\omega}$ and phase shift that deteriorated the discussion. The top and bottom panel of Fig. 3(a) shows, respectively, the zoomed magnitude and phase of $V_{3\omega}$ in a typical measurement. Increasing the frequency led to the decrease in both the measured amplitude and phase ($\phi_{3\omega}$). This in our measurement was however primarily attributed to the parasitic capacitance in circuit, originating from the capacitance of the cable connections in measurement (100 pF/m) and the stray capacitance from differential amplifiers, as indicated in Fig. 3(b). Though they are individually small, the sum of them in circuit can reach 1–1.5 nF. For conventional highly conductive samples, this is not serious due to their low resistance in hundreds Ω and the resulting high RC frequency. However, it is a significant a challenge for measuring semiconductor nanowires with resistance over tens of kΩ to MΩ, which causes poorly guarded current leakage and phase shift issues at higher frequencies that disturb the accurate measurement of the magnitude and phase of $V_{3\omega}$. In our measurement, because of the large resistance of semiconductor Si nanowires (10–200 kΩ), the obtained frequency dependency was artificially deviated by the parasitic effects. This is supported by the simple RC fitting of the phase shift displayed in Fig. 3(a), in which the nanowire resistance (23 kΩ), reference resistor (23 kΩ), and several estimated parasitic capacitance values ($C_p = 0.5$, 1.0, 1.5 nF) were chosen to fit the measurement. The phase shift in measurement at higher frequency (to 400 Hz) was found addressable by the parasitic effect, since they resulted in similar phase shifts. However, we note that under low frequency <100 Hz, the parasitic effect becomes negligible that both the magnitude and phase of $V_{3\omega}$ saturate to constant values in measurements. Under such conditions, a constant thermal conductivity value could be obtained for the investigation of nanowire thermal conductivity.

In our experiment, the Si nanowires exhibit a relatively uniform diameter of 45 ± 5 nm; we therefore primarily varied the length of nanowires in measurements from 400 nm to 4 μm to gain insights into size restricted thermal transport characteristics, which has been utilized to extract the phonon spectra information.[23,24] The results are summarized in Fig. 4(a), in which κ seems to be constant at $L > 2\,\mu$m but shows strong length dependence at $L < 2\,\mu$m. Because the thermal resistance between the nanowire and contact electrode would lead to the underestimation of the inherent thermal conductivity of nanowires, especially for those short nanowires, we first estimated the thermal contact resistance (R_{th_c}) to the nanowire using the total thermal resistance in measurement calculated from measured κ, by $R_{th}=L/\kappa S$, as displayed in Fig. 4(b). The linear extrapolation at $L > 2\,\mu$m, where the nanowire thermal conductivity is almost constant, indicates that the thermal contact resistance is $\sim 8 \times 10^6$ K/W, which accounts for <10% of the overall thermal resistance of short nanowires with $L < 2\,\mu$m and less for longer nanowires. Here, we first consider the thermal conductivity values of δ-modulated B-doped Si nanowires with $L > 2\,\mu$m, since our initial purpose is to study the effect of δ-modulated dopant distribution on the thermal conductivity of nanowires. At such long length scales, the almost constant κ values for different nanowires indicate that the thermal transport is in the diffusive regime with local thermal equilibrium. After the calibration of thermal contact resistance, the inherent thermal conductivity of 45 nm δ-B-doped Si is estimated to be 22–24 W/m K. The results match well with the previously

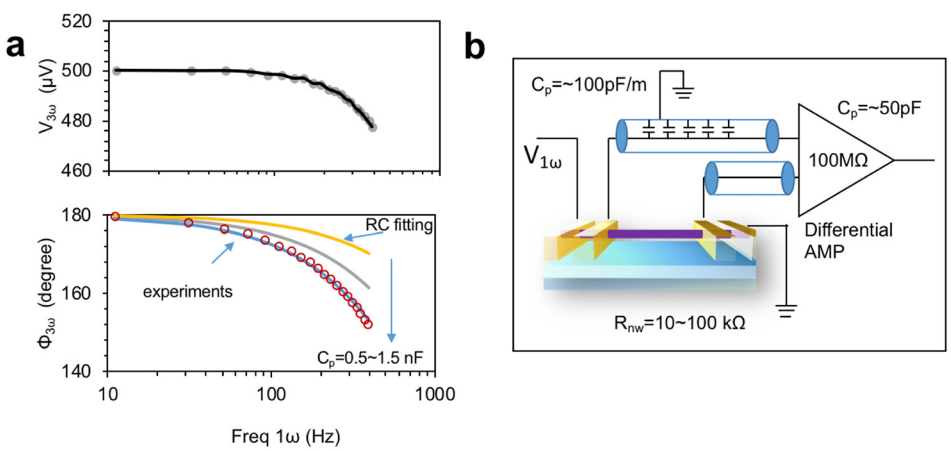

FIG. 3. (a) The amplitude and phase of measured 3ω voltage, the frequency dependency is fitted using the resistance of the nanowire and reference resistor, and the estimated equivalent parasitic capacitance (C_p) from 0.5 to 1.5 nF. (b) The illustration of parasitic capacitance in the measurement circuit connecting to the nanowire device.

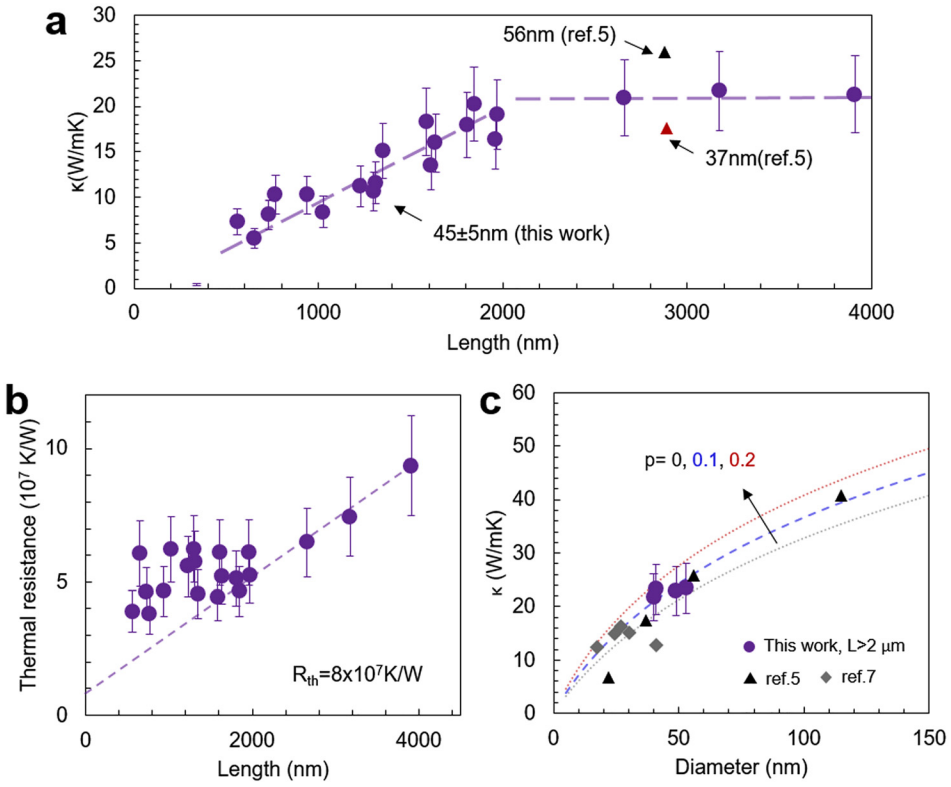

FIG. 4. (a) The measured thermal conductivity of δ-modulated B-doped Si nanowires at varied nanowire lengths and (b) the derived total thermal resistance in device. (c) Comparison of the thermal conductivity of δ-doped Si nanowires to those intrinsic Si nanowires; the data are well fitted using a single specularity $p = 0.1$.

reported values for VLS grown Si nanowires with smooth surfaces[5] and the one with wet etching,[7] as indicated by the summarized diameter dependence in Fig. 4(c). The highly consistent thermal conductivity of present B-doped Si nanowires compared to that without intentional impurity doping suggests that the δ-modulated dopant distribution on the surface of nanomaterials could potentially avoid the unfavorable impurity scattering to phonon transport if one prefers to optimize the thermal dissipation. Such an effect is interpreted by considering the almost diffusive surface scattering to the high frequency phonons that tend to interact with the B impurity atoms. The diffusive surface imposes strong boundary scattering to thermal carrying phonons compared to the impurity effects. Moreover, the confined dopant distribution near the surface also blends impurity scattering into the surface of nanowires, which further limits the effect of impurities on thermal transport.

To elucidate the surface effect to phonon transport, we attempt to extract the surface specularity p by fitting the diameter dependence of nanowire thermal conductivity from our measurement and previous reports by considering the diameter (D) modulation to phonon MFP under Matthiessen's rule[25,26]

$$\frac{1}{\Lambda_{nw}} = \frac{1}{\Lambda_{bulk}} + \frac{1-p}{1+p}\frac{1}{D}, \tag{1}$$

where p is the surface specularity and D is the nanowire diameter. The thermal conductivity of nanowires is calculated by using approximated (BvKS) phonon MFP spectra of bulk Si.[27] As indicated by the dashed lines in Fig. 4(c), the thermal conductivity in all nanowires under diameter confinement is well fitted using $p \approx 0.1$, which indicates the almost diffusive surface for phonons in Si nanowires with an even smooth surface. Although using the singular specularity p for all phonons in Si ignores the frequency dependence of surface scattering,[26] it still qualitatively depicts the diffusive nature of surfaces to the dominant thermal carrying phonons in Si nanostructures, which is likely the result of surface roughness and the interface with surface oxides.[4,11,12] On such a diffusive surface, the presence of impurity atoms will not further influence the thermal conductivity since they do not further redistribute the phonon flux.

Next, we focus on the observed length dependent thermal conductivity at $L < 2\,\mu$m. In Fig. 4(b), the thermal resistance of nanowires at such a length scale seems to exhibit no length dependence. This is distinct from the case of the thermal contact effect in measurements but is similar to the one observed in SiGe nanowires under the ballistic thermal transport,[28,29] in which the conventional Fourier's law tends to fail and the thermal conductance approaches a constant since it depends only on the temperature difference rather than the gradient. To clarify whether the phenomenon is related to the contact effect, we further studied the temperature dependence of the nanowire thermal conductivity at varied length scales.[30] If the thermal resistance in measurement is dominated by the thermal contact, they will then follow the monotonic and linear length dependence at all temperatures.[30] Figure 5 displays the temperature dependence of thermal conductivity and thermal resistance for nanowires from 0.7 to 2.6 μm (note because of the TCR restriction, the κ measurements do not cover the same temperature range). The temperature dependence for long Si nanowires is first found to match well with a previous report,[5] in which κ starts to decrease with T when $T > 150$ K because of increased Umklapp phonon-phonon interaction. For short nanowires of

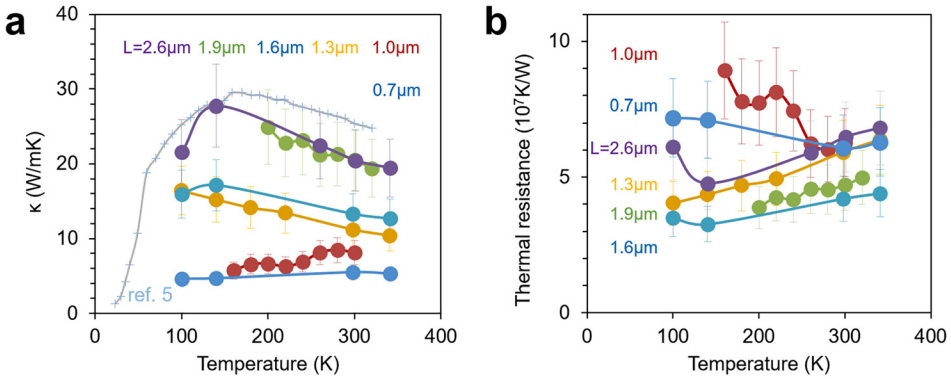

FIG. 5. The temperature dependence of (a) thermal conductivity and (b) thermal resistance for Si nanowires of varied lengths from 0.7 to 2.6 μm.

1 μm and less, κ increases only monotonically with T, implying the suppressed role of Umklapp scattering during phonon transport. When comparing all the measured samples, we found that the thermal resistances for Si nanowires with $L = 0.7$ and $1.0\,\mu$m are close to those with $L = 1.9$ and $2.6\,\mu$m at room temperature and even higher than those at lower T. This contradicts the expectation from thermal contact effect and excludes it from dominating the thermal conductivity in our measurements.

Previously, the length dependent thermal conductivity and resistance observed in SiGe nanowires at an exceptional $8.3\,\mu$m scale were attributed to the ballistic thermal transport; we then examine the potential effect of ballistic transport in the present self-heated Si nanowires. In the case of ballistic thermal transport, the apparent thermal conductivity becomes lower due to the finite thermal flux limited by temperature difference rather than the gradient in the Fourier's law, since the energy of phonons is not dissipated locally due to the absence of scattering [Fig. 6(a)].[24] A suppression function has been generally used to describe the thermal conductivity reduction under such a situation, as $\kappa_{app} = S(\Lambda/L)\kappa_{diff}$, where Λ/L is the Knudsen number that depicts the size confinement to phonons.[27] To obtain the suppression function, the Boltzmann transport equation (BTE) has to be solved to find the thermal flux or temperature profile along the nanowire and compare it to the diffusive situation in Fourier's Law.[31,32] In the case of nanostructured systems like nanowires, the multiple constraints in both the lateral and longitudinal directions have been approximated with simplification based on the Matthiessen's rule that ignores elusive coupling effects.[32] Here, by using the discrete ordinate method (DOM),[33] we solved $S(\Lambda/L)$ for both the micro-thermal bridge method and the present self-heated 3ω method under a set of Knudsen numbers, as displayed in Fig. 6(b). Briefly, the BTE equation with heat generation was expressed in the form of

$$\frac{\partial e(x)}{\partial t} + v \cdot \nabla e(x) = \frac{e_0(x) - e(x)}{\tau} + g(x) \qquad (2)$$

in which v, τ, e, and e_0 are, respectively, the phonon velocity, lifetime, energy, and equilibrium energy and g is the heat generation term. By using the phonon MFP, τ is expressed as $\tau = \Lambda/v$ in the calculation. Following Ref. 33, the equilibrium phonon energy profile along nanowires is solved by using the PDE package of Comsol Multiphysics, with the angular direction of phonon transport discreted by 64 Gaussian quadrature points. In the case of the 3ω method, g is set to be $Q_j/\Omega L$, with Q_j denoting the total heating power Q_j, $\Omega = 4\pi$ the solid angle, and L the nanowire length; in the other case of the micro-thermal bridge method, g is set to 0 at $0 < x < L$ and Q_j/Ω at $x = L$ for a monotonous heat flow. The numerically solved energy profile is then interpreted into nanowire temperature by using the specific heat capacity (C) of energy carrying phonons, as $\Delta T(x) = \int e_0(x) d\Omega/C$, which is further used to calculate the effective thermal conductivity in the framework of Fourier's law. The suppression function is finally obtained by comparing the calculated effective thermal conductivity at varied L/Λ ratios to the intrinsic nanowire thermal conductivity at the diffusive limit ($\kappa_0 = 1/3CV\Lambda$).

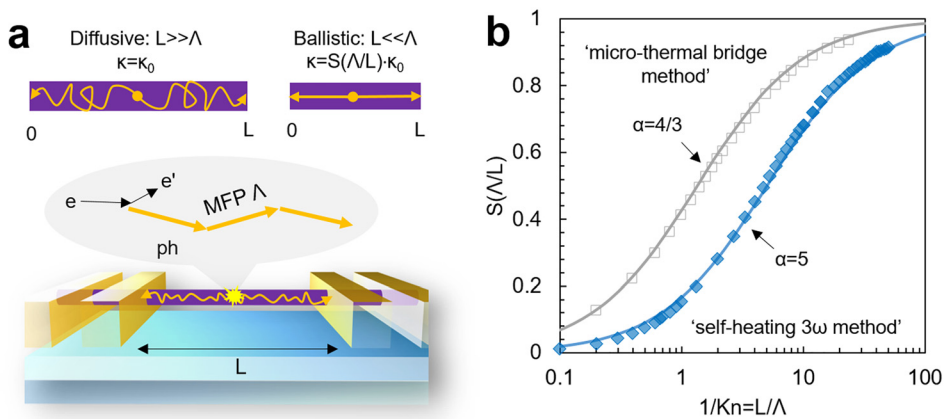

FIG. 6. (a) The illustration of diffusive and ballistic thermal transport in self-heated nanowires and (b) the numerical calculated suppression function for the micro-thermal bridge method and present self-heated 3ω method.

For the conventional micro-thermal bridge method, S(Λ/L) has been analytically solved to have the form

$$S = \frac{1}{1 + \alpha \frac{\Lambda}{L}} \tag{3}$$

with $\alpha \approx 3/4$.[34] Our numerical solution of S(Λ/L) for the micro-thermal bridge method is seen to agree well with the above function, while for the self-heated 3ω method, S(Λ/L) is apparently lower and shifted toward larger L/Λ values, meaning that the ballistic effect would appear at longer lengths in the self-heated 3ω method, which is closely related to the different heat generation profile and the bilateral thermal dissipation along self-heated nanowires.[31] Nevertheless, we note that the suppression to thermal conductivity in the above by the ballistic effect could be interpreted through a virtual thermal resistance at the boundary.[35]

Next, we attempt to use the above suppression function and the grey phonon model that treat phonon transport with an dominant phonon MFP (Λ_{grey}) to interpret the experimental results. Figure 7 displays the fitting to experimental data by using varied Λ_{grey} from 50 to 400 nm and the diffusive thermal conductivity of 22.5 W/m K. The length dependence of measured thermal conductivity at $L > 2\,\mu m$ is well fitted by using smaller MFP values of <100 nm, while the dependence at $L < 2\,\mu m$ is more fitted by longer MFPs of ~400 nm. The discrepancy observed at long and short length limits suggests that the thermal transport in nanowires at varied length scales under the quasi-ballistic regime cannot be directly predicted by the simplified grey phonon model. Hence, it is necessary to adopt the phonon MFP spectra information to understand the spectral effect in the length restricted thermal transport. In this case, the effective thermal conductivity for a nanowire of length L is written as

$$\kappa = \int_{\Lambda=0}^{\infty} \kappa(\Lambda) S(\Lambda/L) d\Lambda\,, \tag{4}$$

where $\kappa(\Lambda)$ is the thermal conductivity contribution by the phonons with MFP Λ. By still using the BvKS approximation of the MFP spectra for Si nanowires,[27] we further model the length dependence of thermal conductivity for Si nanowires by using the interpolated suppression function obtained from the numerical method. The fitting with $p = 0.1$ is seen to resemble well the saturated thermal conductivity at $L > 2\,\mu m$, while the predicted κ is still apparently higher than the experimental results for those short nanowires. One may argue that the adopted MFP spectra for Si nanowires using the singular specularity may underestimate the contribution of low frequency phonons that are likely to have long MFPs in nanowires due to their weak interaction with surface roughness.[36] However, in the grey model that considers only a dominant phonon MFP, we have found that increasing the thermal contribution of long MFP phonons contradicts with the saturated thermal conductivity at $L > 2\,\mu m$, because it will lead to an apparent decrease in nanowire thermal conductivity at much longer nanowire lengths, as indicated by the fitting in Fig. 7. We note that in a recent study which attempts to interpret the experimental results of ballistic thermal transport in SiGe nanowires,[34] a similar discrepancy was also observed between the theoretical modeling and experimental findings. Such a departure indicates that existing modeling of ballistic thermal transport may underestimate the resistive processes that are experienced by phonons.

It is well known that under joule heating, the emitted phonons from electron-phonon interaction are initially in the non-equilibrium states,[37] which then decay immediately to thermal equilibrium through various phonon-phonon interactions (normal and Umklapp processes).[38] However, in the above, the equilibrium phonon MFP spectra were assumed in the estimation of length dependent thermal conductivity. The departure from measurements results can be attributed to the inefficient thermalization of heat carrying phonons that modulate the temperature profile along nanowires under the quasi-ballistic thermal transport,[39] due to the less efficient phonon-phonon interactions implied in the temperature dependence of κ [Fig. 5(a)]. The inefficient thermalization of phonon spectra under the ballistic limit will result in less active phonon modes that carry heat, which leads to the decrease in effective heat capacity and therefore apparently lower thermal conductivity values in measurements. From the perspective of thermal resistance, the discrepancy between equilibrium spectra modeling and the measured data can be understood as the result of ignored phonon resistive processes that are associated with the thermalization of non-equilibrium phonons. By treating the non-equilibrium or hot phonons as relaxons that propagate and decay as a group,[40] we could assign a MFP Λ_{th} to describe the thermalization of these phonons and attempt to quantitatively

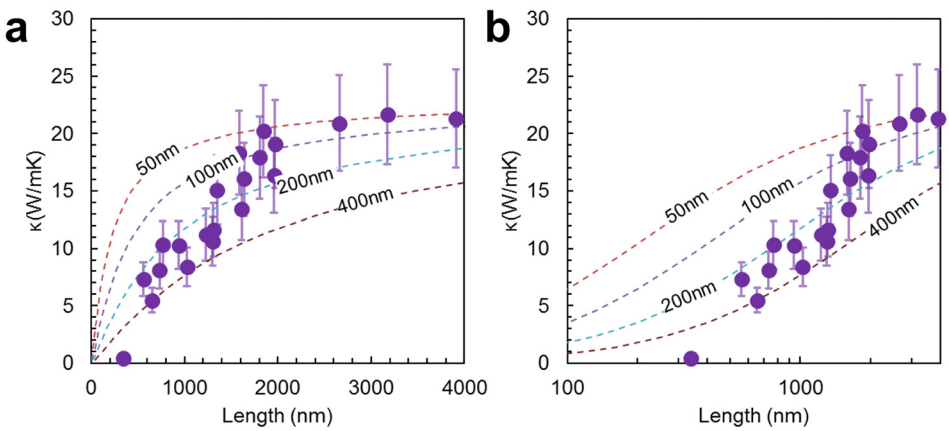

FIG. 7. Interpretation of the length dependent thermal conductivity by a gray phonon model using the numerical calculated suppression function and varied MFP values from 50 to 400 nm: (a) length in linear scale and (b) length in log scale.

interpret the observed length dependence of κ by evaluating the extent of thermalization in nanowires.[39] Considering the classic characteristic of decay processes, where the direct transmission rate of hot phonons to a distance x is $e^{-x/\Lambda th}$, one can find the overall transmission rate for all joule heated phonons along the nanowire to the terminals are

$$\chi(\mathrm{L}, \Lambda_{th}) = \frac{\Lambda_{th}}{L}\left(1 - e^{-\frac{L}{\Lambda_{th}}}\right) \tag{5}$$

which is a function of nanowire length L and the thermalization distance Λ_{th}. When $L \ll \Lambda_{th}$, $\chi \approx 1$ that most phonons directly escape the nanowire without being scattered or thermalized into equilibrium, the heat dissipation flux is then intimately determined by the joule-heat emitted phonon spectra, while when $L \gg \Lambda_{th}$, χ approaches 0 that all the hot phonons are efficiently thermalized with their energy dissipated into local lattice, in which the heat flux could be simply modeled using the equilibrium phonon spectra of the nanowire. By including a thermalization resistance (R_{th}) at the boundary for those ballistic phonons, the overall thermal resistance for phonons in the nanowire of length L could be approximated by treating ballistic and equilibrium phonons separately, as

$$\mathrm{R}(L, \Lambda_{th}) = R_{nw}(L)[1 - \chi(L, \Lambda_{th})] + R_{th}\chi(L, \Lambda_{th}), \tag{6}$$

where $R_{nw}(L) = L/\kappa(L)S$ is the thermal resistance of the nanowire with equilibrium phonon spectra. Using $R_{th} \approx 8 \times 10^7$ K/W and $\Lambda_{th} \approx 400$ nm, we found that the observed length dependence of thermal conductivity in measurements could be well addressed, as displayed in Fig. 8(a). The thermalization MFP for non-equilibrium joule-heating phonons is considerably longer than the diameter or the median MFP estimated for the nanowires. However, it is comparable to the length scale (200 nm) that ballistic thermal transport behavior was observed in holey Si, which has been attributed to be the low-pass filter effect to the equilibrium phonon spectra by surfaces and interfaces in measurements. In our case, this might be related to the non-equilibrium phonon spectra emitted from electron-phonon interaction during joule heating.[38] In a recent study, Raja *et al.* measured the length dependence of the thermal conductivity for heavily Boron doped Si nanowires ($P = 10^{19}$ cm^{-3}),[30] which have the average diameter of 30 nm defined by top-down etching. Though they used a similar self-heated method with a DC source, no apparent length dependence of thermal conductivity was observed in their measurements, which indicated only diffusive thermal transport behavior nanowires as short as 400 nm. The different length dependence might be related to the different thermalization characteristic of joule-heat phonons under diameter restriction and dopant impurity modulation, as they participate actively in the inelastic phonon scattering and thermalization.[41] Note that the phonon thermalization effect in joule-heated systems has been observed in carbon nanotubes[39] with preferentially heated longitudinal optical phonons under electric field.[42] Our present study indicates that the thermal dissipation in the miniaturized Si nanostructure upon joule-heating may also be significantly modulated by the presence of non-equilibrium phonons from electron-phonon interaction. In the future, further experimental study on size dependence and theoretical modeling of the phenomenon that considers detailed electron-phonon interaction would be necessary to gain further insights into the nanoscale thermal dissipation characteristics and their measurements.

CONCLUSION

In summary, we have measured the thermal conductivity of δ-modulated B-doped Si nanowires that exhibit a heavily Boron doped surface. The nanowire thermal conductivity saturates at long nanowire length scales, which are identical to that without dopant impurities. The highly consistent thermal conductivity for Si nanowires with different radial dopant distributions is attributed to the almost diffusive surface to phonons in Si nanowires, as supported by the fitted surface specularity. The results thus shed light on the engineering of dopant distribution in nanostructured electronic devices to avoid the thermal dissipation issues caused by high concentration impurity scattering. Furthermore, we found the abnormal length dependence of thermal conductivity of Si nanowires which is related to the ballistic thermal transport in self-heated 1D nanowires. The phenomenon however could not be explained through the usual equilibrium phonon spectra, but can be addressed by considering the non-equilibrium hot phonons emitted from joule heating and their thermalization during propagation, which is generally ignored in the previous study.

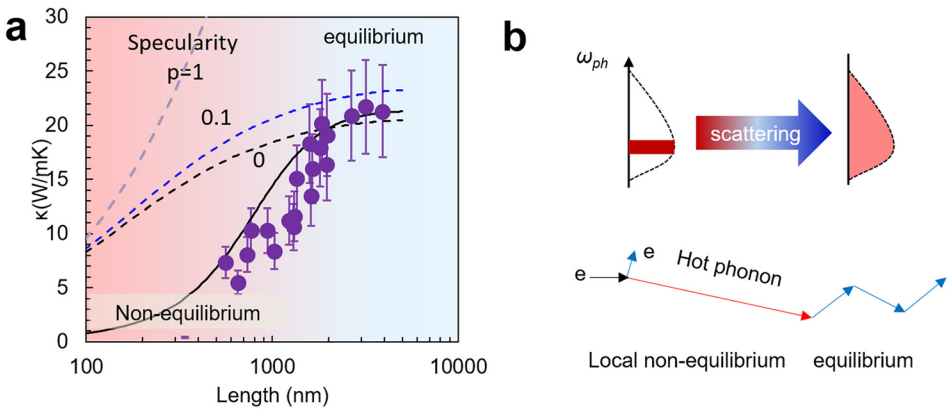

FIG. 8. The fitting to measured length dependence of (a) thermal conductivity using the numerically calculated suppression function and approximated BvKS phonon spectra with varied surface specularity (dashed line). The solid line is fitted by considering the heat flux carried by non-equilibrium phonons from joule-heating and their thermalization resistance. (b) A schematic illustration explaining the resistive processes for phonon escaping the nanowire under quasi-ballistic thermal transport.

ACKNOWLEDGMENTS

This work was supported by KAKENHI (Grant Nos. 17H04927, 18H01831, and 18H05243). Y.T. was supported by ImPACT Program of Council for Science, Technology and Innovation (Cabinet Office, Government of Japan). T.T., K.N., K.U., and T.Y. were supported by JST CREST, Japan (Grant No. JPMJCR1331). This work was performed under the Cooperative Research Program of "Network Joint Research Center for Materials and Devices" and the MEXT Project of "Integrated Research Consortium on Chemical Sciences".

[1]E. Pop, Nano Res. **3**, 147 (2010).
[2]G. Meng, F. Zhuge, K. Nagashima, A. Nakao, M. Kanai, Y. He, M. Boudot, T. Takahashi, K. Uchida, and T. Yanagida, ACS Sens. **1**, 997 (2016).
[3]D. Cahill, P. Braun, G. Chen, D. Clarke, S. Fan, K. E. Goodson, P. Keblinski, W. King, G. Mahan, A. Majumdar, H. Maris, S. Phillpot, E. Pop, and L. Shi, Appl. Phys. Rev. **1**, 011305 (2014).
[4]S. Neogi, S. Reparaz, L. Pereira, B. Graczykowski, M. Wagner, M. Sledzinska, A. Shchepetov, M. Prunnila, J. Ahopelto, C. Sotomayor-Torres, and D. Donadio, ACS Nano **9**, 3820 (2015).
[5]D. Y. Li, Y. Y. Wu, P. Kim, L. Shi, P. D. Yang, and A. Majumdar, Appl. Phys. Lett. **83**, 2934 (2003).
[6]A. I. Boukai, Y. Bunimovich, J. Tahir-Kheli, J. K. Yu, W. A. Goddard III, and J. R. Heath, Nature **451**, 168 (2008).
[7]R. Chen, A. I. Hochbaum, P. Murphy, J. Moore, P. D. Yang, and A. Majumdar, Phys. Rev. Lett. **101**, 105501 (2008).
[8]M. C. Wingert, S. Kwon, M. Hu, D. Poulikakos, J. Xiang, and R. K. Chen, Nano Lett. **15**, 2605 (2015).
[9]A. I. Hochbaum, R. Chen, R. D. Delgado, W. Liang, E. C. Garnett, M. Najarian, A. Majumdar, and P. D. Yang, Nature **451**, 163 (2008).
[10]J. Lim, K. Hippalgaonkar, S. C. Andrews, A. Majumdar, and P. Yang, Nano Lett. **12**, 2475 (2012).
[11]P. N. Martin, Z. Aksamija, E. Pop, and U. Ravaioli, Phys. Rev. Lett. **102**, 125503 (2009).
[12]Y. P. He and G. Galli, Phys. Rev. Lett. **108**, 215901 (2012).
[13]C. Blanc, A. Rajabpour, S. Volz, T. Fournier, and O. Bourgeois, Appl. Phys. Lett. **103**, 043109 (2013).
[14]M. Zebarjadi, G. Joshi, G. Zhu, B. Yu, A. J. Minnich, Y. C. Lan, X. W. Wang, M. S. Dresselhaus, Z. F. Ren, and G. Chen, Nano Lett. **11**, 2225 (2011).
[15]F. Zhuge, T. Yanagida, N. Fukata, K. Uchida, M. Kanai, K. Nagashima, G. Meng, Y. He, S. Rahong, X. Li, and T. Kawai, J. Am. Chem. Soc. **136**, 14100 (2014).
[16]N. Yang, G. Zhang, and B. Li, Nano Lett. **8**, 276 (2008).
[17]B. Liao, B. Qiu, J. Zhou, S. Huberman, K. Esfarjani, and G. Chen, Phys. Rev. Lett. **114**, 115901 (2015).
[18]M. Asheghi, K. Kurabayashi, R. Kasnavi, and K. E. Goodson, J. Appl. Phys. **91**, 5079 (2002).
[19]A. Moore and L. Shi, Mater. Today **17**, 163 (2014).
[20]Y. Pan, G. Hong, S. N. Raja, S. Zimmermann, M. Tiwari, and D. Poulikakos, Appl. Phys. Lett. **106**, 093102 (2015).
[21]L. Lu, W. Yi, and D. L. Zhang, Rev. Sci. Instrum. **72**, 2996 (2001).
[22]T. Y. Choi, D. Poulikakos, J. Tharian, and U. Sennhauser, Appl. Phys. Lett. **87**, 013108 (2005).
[23]A. J. Minnich, Phys. Rev. Lett. **109**, 205901 (2012).
[24]A. J. Minnich, J. A. Johnson, A. J. Schmidt, K. Esfarjani, M. S. Dresselhaus, K. A. Nelson, and G. Chen, Phys. Rev. Lett. **107**, 095901 (2011).
[25]A. Balandin, MRS Bull. **39**, 817 (2014).
[26]J. B. Hertzberg, M. Aksit, O. O. Otelaja, D. A. Stewart, and R. D. Robinson, Nano Lett. **14**, 403 (2014).
[27]F. Yang and C. Dames, Phys. Rev. B **87**, 035437 (2013).
[28]T. K. Hsiao, H. K. Chang, S. C. Liou, M. W. Chu, S. C. Lee, and C. W. Chang, Nat. Nanotechnol. **8**, 534 (2013).
[29]B. W. Huang, T. K. Hsiao, K. H. Lin, D. W. Chiou, and C. W. Chang, AIP Adv. **5**, 053202 (2015).
[30]S. N. Raja, R. Rhyner, K. Vuttivorakulchai, M. Luisier, and D. Poulikakos, Nano Lett. **17**, 276 (2017).
[31]Y. C. Hua and B. Y. Cao, Int. J. Heat Mass Transfer **92**, 995 (2016).
[32]Y. C. Hua and B. Y. Cao, Int. J. Therm. Sci. **101**, 126 (2016).
[33]S. Sihn and A. K. Roy, paper presented at the COMSOL Conference, Boston (2009).
[34]H. Zhang, C. Y. Hua, D. Ding, and A. J. Minnich, Sci. Rep. **5**, 09121 (2015).
[35]Y. Hu, L. Zeng, A. J. Minnich, M. S. Dresselhaus, and G. Chen, Nat. Nanotechnol. **10**, 701 (2015).
[36]J. Lee, J. Lim, and P. Yang, Nano Lett. **15**, 3273 (2015).
[37]S. Sadasivam, M. K. Y. Chan, and P. Darancet, Phys. Rev. Lett. **119**, 136602 (2017).
[38]E. Pop, R. Dutton, and K. E. Goodson, Appl. Phys. Lett. **86**, 082101 (2005).
[39]V. V. Deshpande, S. Hsieh, A. W. Bushmaker, M. Bockrath, and S. B. Cronin, Phys. Rev. Lett. **102**, 105501 (2009).
[40]A. Cepellotti and N. Marzari, Phys. Rev. X **6**, 041013 (2016).
[41]N. Ravichandran and A. J. Minnich, Phys. Rev. B **93**, 035314 (2016).
[42]A. Javey, J. Guo, M. Paulsson, Q. Wang, D. Mann, M. Lundstrom, and H. J. Dai, Phys. Rev. Lett. **92**, 106804 (2004).